

REPORT DOCUMENTATION PAGE			Form Approved OMB NO. 0704-0188		
<p>The public reporting burden for this collection of information is estimated to average 1 hour per response, including the time for reviewing instructions, searching existing data sources, gathering and maintaining the data needed, and completing and reviewing the collection of information. Send comments regarding this burden estimate or any other aspect of this collection of information, including suggestions for reducing this burden, to Washington Headquarters Services, Directorate for Information Operations and Reports, 1215 Jefferson Davis Highway, Suite 1204, Arlington VA, 22202-4302. Respondents should be aware that notwithstanding any other provision of law, no person shall be subject to any penalty for failing to comply with a collection of information if it does not display a currently valid OMB control number.</p> <p>PLEASE DO NOT RETURN YOUR FORM TO THE ABOVE ADDRESS.</p>					
1. REPORT DATE (DD-MM-YYYY)		2. REPORT TYPE New Reprint		3. DATES COVERED (From - To) -	
4. TITLE AND SUBTITLE Electronic tuning of La ₂ /3Sr ₁ /3MnO ₃ thin films via heteroepitaxy			5a. CONTRACT NUMBER W911NF-08-1-0317		
			5b. GRANT NUMBER		
			5c. PROGRAM ELEMENT NUMBER 611103		
6. AUTHORS Franklin J. Wong, Shaobo Zhu, Jodi M. Iwata-Harms, Yuri Suzuki			5d. PROJECT NUMBER		
			5e. TASK NUMBER		
			5f. WORK UNIT NUMBER		
7. PERFORMING ORGANIZATION NAMES AND ADDRESSES University of Iowa @ Iowa City Office of Sponsored Programs The University of Iowa Iowa City, IA 52242 -			8. PERFORMING ORGANIZATION REPORT NUMBER		
9. SPONSORING/MONITORING AGENCY NAME(S) AND ADDRESS(ES) U.S. Army Research Office P.O. Box 12211 Research Triangle Park, NC 27709-2211			10. SPONSOR/MONITOR'S ACRONYM(S) ARO		
			11. SPONSOR/MONITOR'S REPORT NUMBER(S) 54223-MS-MUR.40		
12. DISTRIBUTION AVAILABILITY STATEMENT Approved for public release; distribution is unlimited.					
13. SUPPLEMENTARY NOTES The views, opinions and/or findings contained in this report are those of the author(s) and should not be construed as an official Department of the Army position, policy or decision, unless so designated by other documentation.					
14. ABSTRACT Epitaxial La ₂ /3Sr ₁ /3MnO ₃ films grown on LaAlO ₃ substrates of various orientations exhibit a range of magnetoresistive properties, demonstrating the utility of strain as an electronic tuning parameter for manganites. Large magnetoresistance over a broad range of temperatures—highest (!64% at 50 kOe) at the lowest temperatures measured—is observed in a coherently strained La ₂ /3Sr ₁ /3MnO ₃ film on a (001) LaAlO ₃ substrate. In addition to higher magnetoresistance, its reduced magnetization and					
15. SUBJECT TERMS Electronic tuning, heteroepitaxy					
16. SECURITY CLASSIFICATION OF:			17. LIMITATION OF ABSTRACT UU	15. NUMBER OF PAGES	19a. NAME OF RESPONSIBLE PERSON Michael Flatte
a. REPORT UU	b. ABSTRACT UU	c. THIS PAGE UU			19b. TELEPHONE NUMBER 319-335-0201

Report Title

Electronic tuning of $\text{La}_{2/3}\text{Sr}_{1/3}\text{MnO}_3$ thin films via heteroepitaxy

ABSTRACT

Epitaxial $\text{La}_{2/3}\text{Sr}_{1/3}\text{MnO}_3$ films grown on LaAlO_3 substrates of various orientations exhibit a range of magnetoresistive properties, demonstrating the utility of strain as an electronic tuning parameter for manganites. Large magnetoresistance over a broad range of temperatures—highest (164% at 50 kOe) at the lowest temperatures measured—is observed in a coherently strained $\text{La}_{2/3}\text{Sr}_{1/3}\text{MnO}_3$ film on a (001) LaAlO_3 substrate. In addition to higher magnetoresistance, its reduced magnetization and conductance suggest the stabilization of a more insulating ground state and the possibility of strain-induced phase coexistence. Similar field-dependent magnetotransport features at low temperatures, distinct from those exhibited by bulk manganites, are also seen in a partially strained film on a (110) LaAlO_3 substrate, but bulk-like magnetoresistive behavior is observed in a relaxed $\text{La}_{2/3}\text{Sr}_{1/3}\text{MnO}_3$ film on a (111) LaAlO_3 substrate. VC 2012 American Institute of Physics.

REPORT DOCUMENTATION PAGE (SF298)
(Continuation Sheet)

Continuation for Block 13

ARO Report Number 54223.40-MS-MUR
Electronic tuning of La₂/3Sr₁/3MnO₃ thin films v ...

Block 13: Supplementary Note

© 2012 . Published in Journal of Applied Physics, Vol. Ed. 0 111, (6) (2012), (, (6). DoD Components reserve a royalty-free, nonexclusive and irrevocable right to reproduce, publish, or otherwise use the work for Federal purposes, and to authorize others to do so (DODGARS §32.36). The views, opinions and/or findings contained in this report are those of the author(s) and should not be construed as an official Department of the Army position, policy or decision, unless so designated by other documentation.

Approved for public release; distribution is unlimited.

Electronic tuning of $\text{La}_{2/3}\text{Sr}_{1/3}\text{MnO}_3$ thin films via heteroepitaxy

Franklin J. Wong,^{1,a)} Shaobo Zhu,¹ Jodi M. Iwata-Harms,¹ and Yuri Suzuki^{1,2}¹*Department of Materials Science and Engineering, University of California, Berkeley, California 94720, USA*²*Materials Sciences Division, Lawrence Berkeley National Laboratory, Berkeley, California 94720, USA*

(Received 4 January 2012; accepted 27 February 2012; published online 29 March 2012)

Epitaxial $\text{La}_{2/3}\text{Sr}_{1/3}\text{MnO}_3$ films grown on LaAlO_3 substrates of various orientations exhibit a range of magnetoresistive properties, demonstrating the utility of strain as an electronic tuning parameter for manganites. Large magnetoresistance over a broad range of temperatures—highest (−64% at 50 kOe) at the lowest temperatures measured—is observed in a coherently strained $\text{La}_{2/3}\text{Sr}_{1/3}\text{MnO}_3$ film on a (001) LaAlO_3 substrate. In addition to higher magnetoresistance, its reduced magnetization and conductance suggest the stabilization of a more insulating ground state and the possibility of strain-induced phase coexistence. Similar field-dependent magnetotransport features at low temperatures, distinct from those exhibited by bulk manganites, are also seen in a partially strained film on a (110) LaAlO_3 substrate, but bulk-like magnetoresistive behavior is observed in a relaxed $\text{La}_{2/3}\text{Sr}_{1/3}\text{MnO}_3$ film on a (111) LaAlO_3 substrate. © 2012 American Institute of Physics. [<http://dx.doi.org/10.1063/1.3699047>]

I. INTRODUCTION

In the colossal magnetoresistive perovskite manganites, the charge, orbital, and spin degrees of freedom are strongly coupled to the lattice state, making them sensitive to epitaxial lattice perturbations. Although there have been numerous magnetotransport studies of manganite thin films,^{1–6} the potential of epitaxial strain as a tuning parameter to traverse electronic phase boundaries has not been fully explored. Both the magnitude and symmetry of strain can be tuned in epitaxial manganite films via substrate choice and orientation and lead to non-bulk-like lattice states.

Bulk manganites exhibit various ordered phases—including ferromagnetic, antiferromagnetic, and charge-ordered—as well as metal/insulator coexistence, which can be promoted by quenched disorder,^{7,8} at both the nanoscopic^{7,9,10} and mesoscopic^{7,9,11–13} length scales. In relatively small electronic bandwidth manganites, charge-ordered insulator to ferromagnetic metal transitions can be induced by an applied magnetic field.^{8,14} In these cases, high magnetoresistance (MR) values are observed at temperatures well below the Curie temperature (T_c) or the charge ordering temperature. In other manganites that exhibit temperature-induced ferromagnetic metal to paramagnetic insulator transitions, the coexistence of a paramagnetic polaronic phase with a ferromagnetic metallic phase is expected to be important for explaining their colossal MR (CMR) in the vicinity of their magnetic transitions.^{15–18}

Not all alloys of manganites have equally rich phase diagrams but, in general, lattice effects on electronic bandwidth are vital to the phenomenology of CMR.⁸ Unlike in the narrower bandwidth manganites, there is no clear evidence for a commensurate charge-ordered state in any alloy of $\text{La}_{1-x}\text{Sr}_x\text{MnO}_3$.^{19,20} Bulk $\text{La}_{2/3}\text{Sr}_{1/3}\text{MnO}_3$, in particular,

undergoes only a ferromagnetic metal to paramagnetic metal transition. Its low-temperature double-exchange ferromagnetic phase appears to be very stable, and it has a relatively high T_c . Therefore, it exhibits comparatively unspectacular magnetoresistive properties, making it an ideal system to study the potential of engineering MR through epitaxial strain. Although its bulk ground state is not near a metal/insulator phase boundary, there have been studies of epitaxial $\text{La}_{2/3}\text{Sr}_{1/3}\text{MnO}_3$ films that suggest strain-stabilized low-temperature insulating phases^{1,4,21,22} and possible phase coexistence.²² Similar observations have been reported in ultrathin $\text{La}_{2/3}\text{Sr}_{1/3}\text{MnO}_3$ films,²³ and at the film/substrate interface of Ca-based manganite thin films.²⁴ Nevertheless, the relationship between strain-induced phase competition and CMR in $\text{La}_{2/3}\text{Sr}_{1/3}\text{MnO}_3$ films have yet to be thoroughly investigated experimentally.

In this study, by growing $\text{La}_{2/3}\text{Sr}_{1/3}\text{MnO}_3$ films on different orientations of LaAlO_3 (LAO) substrates, we vary the magnitude and sign of the thin-film strain tensors, accessing lattice states not achievable in bulk. We observe marked phenomenological differences in magnetotransport of these films compared to that of bulk alloyed manganites. Other transport studies of strained thin-film $\text{La}_{2/3}\text{Sr}_{1/3}\text{MnO}_3$ have focused primarily on strain-induced modifications to T_c in (001) films.^{1,25,26} In the coherently strained $\text{La}_{2/3}\text{Sr}_{1/3}\text{MnO}_3$ film on a (001) LAO substrate, we report MR at 50 kOe in excess of −35% over the entire temperature regime below 250 K. The partially strained (110) film has smaller low-temperature MR of roughly −10%, but still much higher than expected in the bulk. The relaxed (111) film shows more bulk-like behavior with significant MR only near T_c . Our results demonstrate that the MR in $\text{La}_{2/3}\text{Sr}_{1/3}\text{MnO}_3$ thin films can be enhanced and the operative temperature range broadened compared to the bulk, and they can exhibit temperature- and field-dependent behavior unique from bulk manganites of any stoichiometry. They further suggest the possibility of strain-stabilized low-temperature phase coexistence.

^{a)}Author to whom correspondence should be addressed. Electronic mail: franklin_wong@berkeley.edu.

II. EXPERIMENTAL

We deposited 34 nm thick $\text{La}_{2/3}\text{Sr}_{1/3}\text{MnO}_3$ thin films on (001), (110), and (111) LAO substrates using pulsed-laser deposition with a KrF excimer laser operating at 10 Hz and $\sim 1 \text{ J/cm}^2$ on a stoichiometric, powder-pressed target. The films were deposited at 700°C , in 320 mTorr of O_2 , and subsequently cooled to room temperature in 300 Torr of O_2 . The stoichiometry and thickness of the films were measured with Rutherford backscattering spectrometry. X-ray diffraction was performed on a Panalytical X'Pert diffractometer. The ω scans of the out-of-plane peaks for the (001), (110), and (111) substrates are aligned such that ω is the angle between the x-ray beam and the in-plane [010], $[\bar{1}\bar{1}0]$, and $[\bar{1}\bar{1}2]$ directions of the substrate, respectively. Pseudocubic Miller indices are used to reference crystallographic planes and directions. Magnetic measurements were performed in a Quantum Design SQUID magnetometer. Electrical transport measurements were performed in the van der Pauw geometry with Au-Pd contacts deposited onto the corners of the samples in a Quantum Design Physical Property Measurement System. Magnetotransport measurements were performed with the field applied normal to the sample plane.

III. RESULTS AND DISCUSSION

Structural characterization indicates that we have synthesized highly crystalline epitaxial $\text{La}_{2/3}\text{Sr}_{1/3}\text{MnO}_3$ thin films. X-ray diffraction measurements, including 2θ - θ (data not shown) and ω scans of the out-of-plane reflections [Fig. 1(a)], were performed on all films. The ω scan full-width at half-maximum values of the out-of-plane reflections [Table I] indicate that the (110) film has the best in-plane crystalline quality and the (111) film has the largest mosaic spread.

TABLE I. Properties of the 34 nm heteroepitaxial (001), (110), and (111) films. d refers to the spacing between (hkl) planes of the corresponding (hkl) films, and the interplanar spacings are compared to those of the bulk. Bulk interplanar spacing values are calculated using the pseudocubic lattice parameter of 3.88 \AA . The measured full-width at half-maximum (FWHM) values are from ω scans in Fig. 1(a). The saturated magnetic moment (M_S) is measured at 7 K, MR at 10 K and 50 kOe, and resistivity (ρ) at 10 K.

Sample	d_{film} (\AA)	d_{bulk} (\AA)	FWHM ($^\circ$)	M_S (μ_B/Mn)	T_c (K)	MR (%)	ρ ($\text{m}\Omega\text{-cm}$)	ρ (273 K)/ ρ (10 K)
(001)	3.99	3.88	0.18	2.49	325	-64	1.69	2.92
(110)	2.77	2.745	0.11	3.48	334	-10	0.227	8.04
(111)	2.25	2.24	0.33	3.53	347	-1	0.117	7.81

Reciprocal space maps (RSMs) of the 103 reflection of the (001) film, the 312 reflection of the (111) film, and the 221 and 310 reflections of the (110) film were taken to determine the in-plane (in)coherency between the film and substrate [Figs. 1(b)-1(e)]. From Fig. 1(b), we see that the (001) film is strained coherently and assumes a tetragonal structure. On the other hand, the (111) film is nearly completely relaxed [Fig. 1(c)], and the out-of-plane (111) interplanar spacing is found to be almost equal to that of the bulk [Table I]. The (110) film is coherently strained along the in-plane [001] direction [Fig. 1(d)], but is almost fully relaxed along the $[\bar{1}\bar{1}0]$ direction [Fig. 1(e)]. It appears that coherent strain can be more easily maintained if the stress is applied along a direction of only principal components.

In terms of the magnetic properties, the (001) film has a magnetically easy [001] direction, the (110) film has a magnetically easy $[\bar{1}\bar{1}0]$ direction, and the (111) film has an easy (111) plane. The observed magnetic anisotropy in the (001) and (110) films is consistent with that reported by Berndt

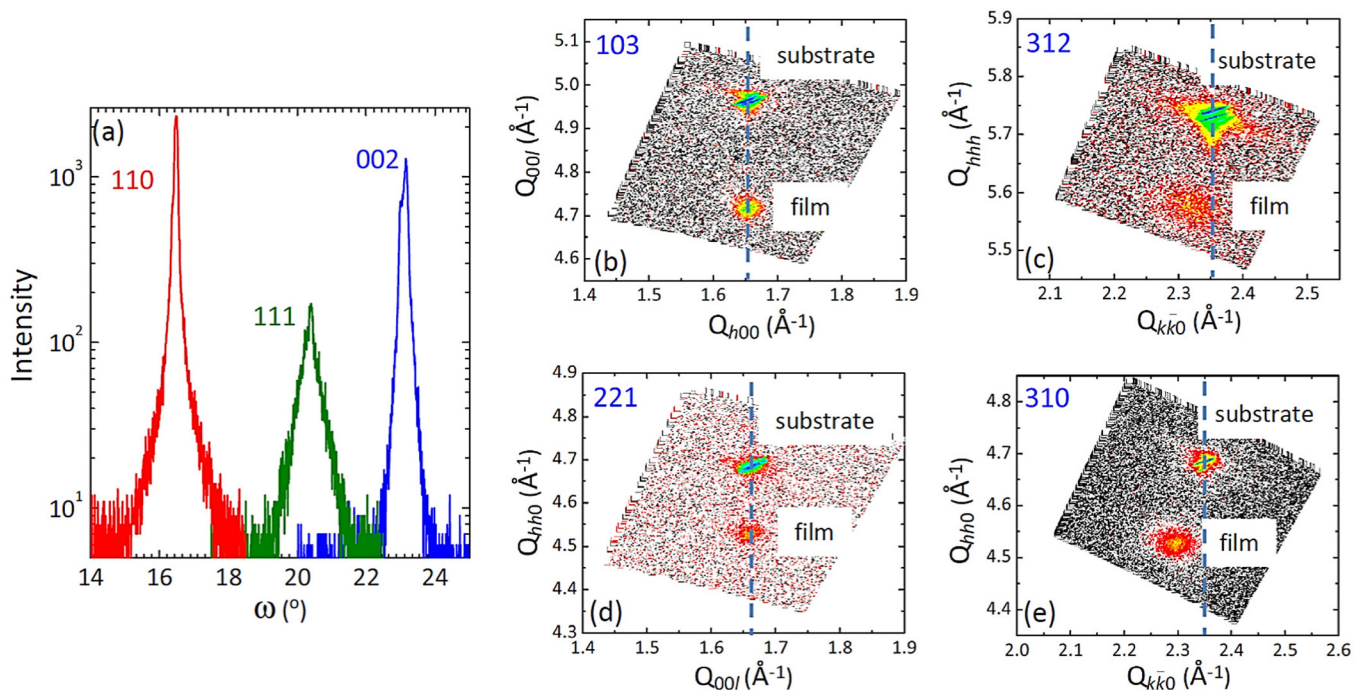


FIG. 1. (a) ω scans of the 002, 110, and 111 reflections of the (001), (110), and (111) films, respectively. Antisymmetric x-ray diffraction scans of the (b) 103 reflection of the (001) film, (c) the 312 reflection of the (111) film, (d) the 221 and (e) 310 reflections of the (110) film. Reciprocal space coordinates Q are defined as 2π divided by real space distances. The vertical lines help guide the eye.

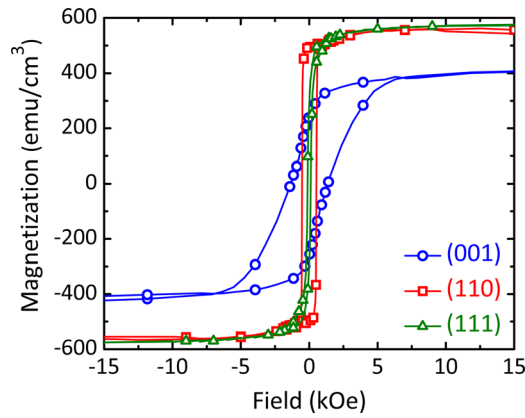


FIG. 2. Hysteresis loops measured at 7 K of the (001), (110), and (111) films. The expected saturated magnetization value of the bulk material is 587 emu/cm^3 .

*et al.*²⁷ Magnetic hysteresis loops of the samples at 7 K were taken along their respective easy directions (plane) [Fig. 2]. The (001) film has the lowest saturated magnetization of 401 emu/cm^3 , or $2.49 \mu_B/\text{Mn}$. The partially strained (110) film and the nearly fully relaxed (111) film show a saturated magnetization of 553 emu/cm^3 ($3.48 \mu_B/\text{Mn}$) and 561 emu/cm^3 ($3.53 \mu_B/\text{Mn}$), respectively; these values are close to the expected saturated magnetization of 587 emu/cm^3 , assuming $3.67 \mu_B/\text{Mn}$.

The temperature-dependent remnant magnetization values normalized to those at 7 K along the easy directions (plane) are shown in Fig. 3(a); the scans were taken in zero field after field cooling the samples in 10 kOe. We measured the remnant magnetization to get a better estimate of the T_c 's, at which the remanence disappears, so that the T_c 's are not smeared by an applied field. Compared to the bulk T_c of $\sim 355 \text{ K}$, the (001) film has a suppressed T_c of 325 K , the (110) film has a slightly suppressed T_c of 334 K , and the (111) film displays a T_c of 347 K . Despite comparable saturation magnetization values of the (110) and (111) films, the lower T_c of the (110) film is an indication of weaker ferromagnetic exchange interactions. The nearly unstrained (111) film is the most similar to the bulk.

The $\text{La}_{2/3}\text{Sr}_{1/3}\text{MnO}_3$ films grown on (110) and (111) substrates show metal-like temperature-dependent resistivity up to 385 K [Fig. 3(b)], akin to the bulk phase of this stoichiometry. However, the (001) film exhibits insulator-like behavior at high temperatures, and the sheet resistance maximum at $\sim 295 \text{ K}$ resembles a metal-insulator transition. More importantly, the low-temperature resistivity of the (001) film is about an order of magnitude larger than those of the (110) and (111) films. Figures 3(b) and 3(c) show the resistivity curves of the films measured in zero field and 50 kOe as well as the corresponding MR at 50 kOe: $(\rho_{50 \text{ kOe}} - \rho_{0 \text{ kOe}}) / \rho_{0 \text{ kOe}}$. In Figs. 3(b) and 3(c), the temperature was swept from high to low, so the samples were field cooled. Magnetization and resistivity scans of all of our samples did not exhibit any temperature hysteresis.

The fully relaxed $\text{La}_{2/3}\text{Sr}_{1/3}\text{MnO}_3$ film on the (111) LAO substrate shows a peak in MR at 351 K , near its T_c of 347 K , as observed in the bulk material of the same stoichiometry. Though the peak in MR of the (110) film likewise

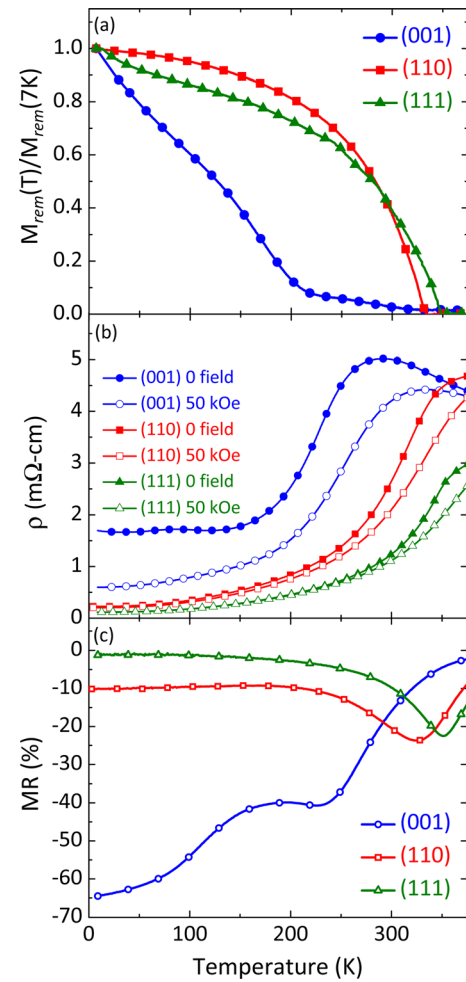


FIG. 3. (a) Remnant magnetization (M_{rem}) normalized to the value at 7 K, (b) temperature-dependent resistivity (ρ) at zero field (solid symbols) and 50 kOe (open symbols), and (c) MR of the (001), (110), and (111) films.

occurs near its magnetic transition, it is much broader in temperature range compared to that of the (111) film. In contrast, the (001) film displays high MR over a wide temperature range and reaches its maximum MR at the lowest temperatures measured, whereas the low-temperature MR is negligible in the bulk of the same stoichiometry. The local MR maximum for the (001) film at about 230 K does not correlate with the T_c or the resistivity maximum; however, it does appear to roughly coincide with the increase in remnant magnetization observed below 210 K [Fig. 3(a)]. The MR at 10 K and 50 kOe for the three films are given in Table I.

The resistivity values at 10 K along with the resistivity ratio between the 273 and 10 K values ($\rho_{273 \text{ K}} / \rho_{10 \text{ K}}$) of the films are tabulated in Table I. Upon comparison with x-ray diffraction data, it is not surprising that the (110) film with the sharpest peak in its ω scan [Fig. 1(a) and Table I] also has the highest resistivity ratio. However, the resistivity ratio of the (111) film, which has the greatest crystalline mosaic spread and hence highest degree of structural defects, is comparable to that of the (110) film and much larger than that of the (001) film. We conclude that microstructural defects are not the primary cause of the suppressed T_c , lower magnetization, higher low-temperature

resistivity, and higher peak MR of the (001) film. Furthermore, our data indicate that despite microstructural defects, the higher conductivity of the (111) film may be attributed to greater overlap of the e_g states, which in turn is also responsible for its higher T_c . These observations suggest that atomic lattice distortions are responsible for the differences in magnetic and transport properties.

To examine the low-temperature MR of the (001) film further, we measured the field-dependent resistivity at 7 K [Fig. 4(a)]. The film was heated to 380 K, above its T_c , and subsequently cooled to 7 K in zero field; the magnetic field was increased from zero to positive fields, and the field values were swept in the manner shown by the arrows in Fig. 4(a). In addition to the surprisingly large MR, we also observed other unexpected features: (1) the MR hysteresis does not close up to a field of 70 kOe, while the magnetization versus field measurements do not exhibit any hysteresis at such high

fields; (2) not only is the MR hysteretic, the resistivity change from the initial zero-field value is irreversible with applied magnetic field. The second feature has also been reported by Mukhopadhyay *et al.* in coherently strained $\text{La}_{2/3}\text{Sr}_{1/3}\text{MnO}_3$ thin films on (001) SrTiO_3 , where the tetragonal distortion has the opposite sign,²² but has not been observed in bulk manganites. Interestingly enough, such field-dependent resistivity features are observed in $(\text{LaMnO}_3)_m/(\text{SrMnO}_3)_n$ (for $m=2,3$),⁵ and in $\text{Nd}_{2/3}\text{Sr}_{1/3}\text{MnO}_3/\text{Nd}_{1/2}\text{Ca}_{1/3}\text{MnO}_3$ heterostructures.⁶ In both of these studies, the magnetotransport features are attributed to interfacial effects, but heteroepitaxy-induced phase competition is the underlying theme—as in our case. The irreversibility of the initial zero-field state upon applied fields can be further illustrated by comparing the temperature dependence of resistivity with and without field cooling [Fig. 4(b)]. The temperature was swept from low to high. Field cooling makes the sample more conductive at low temperatures, but the resistivity values are essentially the same above ~ 170 K to within 1% difference. Coincidentally at about this temperature range—well below the T_c of the (001) film—we also observe unexpectedly precipitous changes in its remnant magnetization [Fig. 3(a)]. The initial zero-field resistivity value can be recovered after heating the sample to above its T_c followed by cooling in zero field.

The low-temperature MR of the (110) film exhibits magnetoresistive behavior similar to that of the (001) film, though at considerably lower values. More specifically, the low-temperature MR of the (110) film exhibits hysteretic MR and irreversibility from its initial zero-field state [Fig. 4(b)]. Not only are these MR features distinct from canonical double-exchange, large-bandwidth manganites, but also the field-dependent low-temperature MR characteristics of both the (001) and (110) films are not observed in the small-bandwidth bulk manganites that undergo sharp charge-ordered to ferromagnetic transitions with an applied magnetic field.¹⁴ Also, despite similar temperature dependence of MR to that observed in polycrystalline samples,^{28,29} our strained films exhibit MR with very different field dependence. Our coherently strained (001) and partially strained (110) films exhibit MR features not only different from any La : Sr alloy manganite, but also distinct from all other bulk alloy manganites—single crystalline or polycrystalline. Therefore, the features in our magnetotransport data lead us to believe that indeed heteroepitaxial strain can induce a ground state not achievable in the bulk and perhaps the coexistence of electronic phases.

In order to understand the role of the symmetry of epitaxial lattice distortions on the MR, we evaluate the strain tensors of the (001) and (110) $\text{La}_{2/3}\text{Sr}_{1/3}\text{MnO}_3$ films. Lattice parameters of the films are obtained from the RSMs, and we use the pseudocubic bulk lattice parameter of 3.88 \AA as the reference. Decomposed to represent volume dilation and tetragonal distortion, the strain tensor of the (001) film is

$$\epsilon^{(001)} = -0.63I\% + \begin{bmatrix} -1.69 & 0 & 0 \\ 0 & -1.69 & 0 \\ 0 & 0 & 3.39 \end{bmatrix} \%,$$

where I is the 3×3 identity matrix. Similarly, the strain tensor of the (110) film is

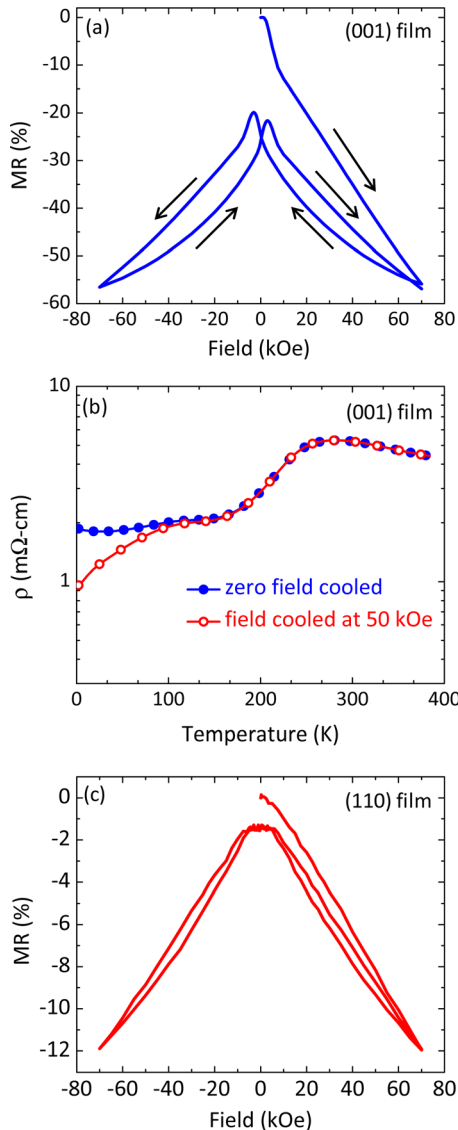


FIG. 4. (a) Field-dependent MR of the coherently strained (001) film at 7 K. (b) Comparison of the zero-field-cooled and field-cooled temperature-dependent resistivity of the (001) film. The sample was heated to 380 K prior to cooling. (c) Field-dependent MR of the partially strained (110) film at 7 K. The field is applied normal to the sample plane.

$$\begin{aligned} \epsilon^{(110)} = & -0.57 I\% + \begin{bmatrix} 0.88 & 0 & 0 \\ 0 & 0.88 & 0 \\ 0 & 0 & -1.75 \end{bmatrix} \% \\ & + \begin{bmatrix} 0 & 0.64 & 0 \\ 0.64 & 0 & 0 \\ 0 & 0 & 0 \end{bmatrix} \%, \end{aligned}$$

where the last component represents shear strain. The breadth of the 312 reflection of the (111) film makes it difficult to perform a similar analysis of its strain tensor. Regardless, both the 2θ - θ and RSM scans suggest that the (111) film is almost fully relaxed.

Comparing the strain tensors of the (001) and (110) films, we see that their volume contractions are comparable. Hydrostatic pressure measurements on bulk samples have shown that the T_c of $\text{La}_{2/3}\text{Sr}_{1/3}\text{MnO}_3$ increases with pressure.³⁰ We do not expect the small difference between the volume contractions of (001) and (110) films to account for the differences in their magnetic and electrical properties; moreover, we observe decreased rather than increased T_c 's. Therefore, the deviatoric strain components are the more crucial parameters that govern the behavior of our films. The tetragonal distortion of the (110) film is not only smaller in magnitude but also opposite in sign to that of the (001) film.

The $\sim 30\%$ lower saturated magnetization and roughly fourteen-fold higher resistivity of the (001) film as compared to the (111) film at low temperatures [Table I] can be attributed to one of two possibilities: (1) a single "ferromagnetic" phase with a canted moment structure, giving rise to reduced conductance, or (2) phase coexistence of a ferromagnetic metallic phase and an insulating, possibly antiferromagnetic, phase. The observation of large low-temperature MR values in the (001) film itself does not rule out either possibility, since the applied magnetic field can reduce canting in the first scenario and induce an insulator-metal metamagnetic transition in the second scenario to account for increased conductivity. However, in a single-phase material, we would expect a more pronounced MR signature near the magnetic transition of the (001) film at 325 K; such a feature is nonexistent in the MR curve of the (001) film [Fig. 3(c)]. In the (111) film, we see a peak in MR near its T_c , characteristic of a single-phase double-exchange ferromagnet.

The (110) film exhibits intermediate behavior; it has a lower degree of tetragonal distortion compared to the (001) film along with some shear strain. Its MR peak is much broader than that of the (111) film. Furthermore, the sizable low-temperature MR of approximately -10% observed in the (110) film suggests that it may be closer to a phase coexistence boundary than the bulk material; this is consistent with its slightly suppressed T_c . We speculate that it may contain some regions of an insulating low-temperature phase that can account for the MR observed at low temperatures. Though much lower in magnitude, the field-dependent low-temperature MR of the (110) film resembles that of the (001) film despite the opposite signs of their respective tetragonal strain tensors. In general, any lattice distortion that acts to reduce the overlap integral of the e_g states in manganites can move the system closer to the metal/insulator phase boundary from

the itinerant side and effectively makes the ferromagnetic state less stable with respect to a low-temperature insulating state; this insulating phase can undergo phase instability upon application of a magnetic field, accounting for low-temperature MR. The observations presented here are also consistent with previous studies that have shown that insulating (001) $\text{La}_{2/3}\text{Sr}_{1/3}\text{MnO}_3$ thin films can be achieved through both in-plane biaxial compression^{1,22} and tension.²² Moreover, A. Tebano *et al.* reported strain-induced orbital polarization of the e_g states from x-ray linear dichroism and evidence of phase separation from nuclear magnetic resonance in strained $\text{La}_{2/3}\text{Sr}_{1/3}\text{MnO}_3$ films on LaAlO_3 .³¹

However, unlike the small-bandwidth manganites that can undergo sharp charge-ordered to ferromagnetic transitions, the field-dependent MR curves at low temperatures of both the (001) and (110) films [Figs. 4(a) and 4(c)] do not show any abrupt changes; we conclude that any possible metamagnetic transition must be gradual. Moreover, the irreversibility of the zero-field resistivity with magnetic field shown in Figs. 4(a) and 4(c) may suggest that the initial electronic state is metastable, and Fig. 4(b) further implies that in the (001) film, the metastability regime occurs below roughly 170 K. Further investigation is necessary to verify the possible (meta)stability of electronic phases in strained manganite films. All in all, deviatoric strain through heteroepitaxy can effectively modify phase competition and magnetic stability in the manganites, as investigated in Colizzi *et al.*'s computational study.³²

We cannot completely rule out the possible effects of thin-film microstructure, but we argue that it plays at most a second-order role. LAO has a rhombohedrally distorted structure and is prone to twin boundaries.³³ Film twinning can be seen in the ω scan of the 002 reflection of the (001) film [Fig. 1(a)]. In fact, ω scans of the 002 reflection across a range of ϕ angles reveal that the film grows almost completely in registry with the twinned substrate (data not shown). However, the strain values associated with the rhombohedral distortion itself³³ and across twin boundaries³⁴ are much lower in magnitude compared to the lattice distortions associated with heteroepitaxy, as signified by $\epsilon^{(001)}$ and $\epsilon^{(110)}$. Furthermore, despite its mosaic spread, the (111) film does not show any MR signature of randomly polycrystalline samples.^{28,29} Therefore, we expect heteroepitaxial lattice distortions, rather than thin-film microstructure, to play the primary role in determining the magnetic and magnetoresistive properties of our films.

IV. CONCLUSION

Despite its reduced saturated magnetization, T_c , and conductivity, the (001) film exhibits remarkably large MR over a wide temperature range. Our findings are particularly surprising because enhanced low-temperature MR is realized in a manganite whose composition in the bulk shows no propensity toward electronic phase coexistence. Therefore, it appears that thin-film lattice distortions can be utilized in lieu of chemical composition to generate equally rich phase diagrams and to engineer MR properties of manganites. We believe epitaxial strain is a promising avenue to traverse

different electronic states of correlated electron systems and therefore to design their macroscopic properties.

ACKNOWLEDGMENTS

We thank K. M. Yu for help with Rutherford backscattering measurements. F.J.W. was supported by the Army Research Office under Grant No. MURI W911NF-08-1-0317. S.Z. and J.M.I. were supported by the National Science Foundation under Grant Nos. 0604277 and 1104401. Initial studies and the X-ray diffraction facility instrument were supported by the Director, Office of Science, Office of Basic Energy Sciences, of the U.S. Department of Energy under Contract No. DE-AC02-05CH11231.

- ¹Y. Takamura, R. V. Chopdekar, E. Arenholz, and Y. Suzuki, *Appl. Phys. Lett.* **92**, 162504 (2008).
- ²T. S. Santos, S. J. May, J. L. Robertson, and A. Bhattacharya, *Phys. Rev. B* **80**, 155114 (2009).
- ³Z. Huang, G. Gao, Z. Yin, X. Feng, Y. Chen, X. Zhao, J. Sun, and W. Wu, *J. Appl. Phys.* **105**, 113919 (2009).
- ⁴A. Tebano, A. Orsini, D. Di Castro, P. G. Medaglia, and G. Balestrino, *Appl. Phys. Lett.* **96**, 092505 (2010).
- ⁵H. Yamada, P.-H. Xiang, and A. Sawa, *Phys. Rev. B* **81**, 014410 (2010).
- ⁶J. Laverdière, S. Jandl, and P. Fournier, *Phys. Rev. B* **84**, 104434 (2011).
- ⁷A. Moreo, M. Mayr, A. Feiguin, S. Yunoki, and E. Dagotto, *Phys. Rev. Lett.* **84**, 5568 (2000).
- ⁸Y. Tokura, *Rep. Prog. Phys.* **69**, 797 (2006).
- ⁹V. B. Shenoy, D. D. Sarma, and C. N. R. Rao, *Chem. Phys. Chem.* **7**, 2053 (2006).
- ¹⁰C. Şen, G. Alvarez, and E. Dagotto, *Phys. Rev. Lett.* **98**, 127202 (2007).
- ¹¹M. Uehara, S. Mori, C. H. Chen, and S.-W. Cheong, *Nature* **399**, 560 (1999).
- ¹²P. G. Radaelli, R. M. Ibberson, D. N. Argyriou, H. Casalta, K. H. Andersen, S.-W. Cheong, and J. F. Mitchell, *Phys. Rev. B* **63**, 172419 (2001).
- ¹³T. Z. Ward, S. Liang, K. Fuchigami, L. F. Yin, E. Dagotto, E. W. Plummer, and J. Shen, *Phys. Rev. Lett.* **100**, 247204 (2008).
- ¹⁴M. Tokunaga, N. Miura, Y. Tomioka, and Y. Tokura, *Phys. Rev. B* **57**, 5259 (1998).
- ¹⁵A. J. Millis, *Nature* **392**, 147 (1998).
- ¹⁶A. J. Millis, T. Darling, and A. Migliori, *J. Appl. Phys.* **83**, 1588 (1998).
- ¹⁷M. Jaime, P. Lin, S. H. Chun, M. B. Salamon, P. Dorsey, and M. Rubinstein, *Phys. Rev. B* **60**, 1028 (1999).
- ¹⁸A. S. Alexandrov, A. M. Bratkovsky, and V. V. Kabanov, *Phys. Rev. Lett.* **96**, 117003 (2006).
- ¹⁹A. Urushibara, Y. Moritomo, T. Arima, A. Asamitsu, G. Kido, and Y. Tokura, *Phys. Rev. B* **51**, 14103 (1995).
- ²⁰H. Fujishiro, M. Ikebe, and Y. Konno, *J. Phys. Soc. Jpn.* **67**, 1799 (1998).
- ²¹E. S. Vlahov, K. A. Nenkov, T. I. Donchev, and A. Y. Spasov, *Vacuum* **69**, 255 (2003).
- ²²S. Mukhopadhyay, I. Das, and S. Banerjee, *J. Phys.: Condens. Matter* **21**, 026017 (2009).
- ²³B. Kim, D. Kwon, T. Yajima, C. Bell, Y. Hikita, B. G. Kim, and H. Y. Hwang, *Appl. Phys. Lett.* **99**, 092513 (2011).
- ²⁴M. Bibes, S. Valencia, B. Martinez, J. Fontcuberta, M. Wojcik, S. Nadolski, and E. Jedryka, *Phys. Rev. B* **66**, 134416 (2002).
- ²⁵F. Tsui, M. C. Smoak, T. K. Nath, and C. B. Eom, *Appl. Phys. Lett.* **76**, 2421 (2000).
- ²⁶C. Adamo, X. Ke, H. Q. Wang, H. L. Xin, T. Heeg, M. E. Hawley, W. Zander, J. Schubert, P. Schiffer, D. A. Muller, L. Maritato, and D. G. Schlom, *Appl. Phys. Lett.* **95**, 112504 (2009).
- ²⁷L. M. Berndt, V. Balbarin, and Y. Suzuki, *Appl. Phys. Lett.* **77**, 2903 (2000).
- ²⁸H. Y. Hwang, S.-W. Cheong, N. P. Ong, and B. Batlogg, *Phys. Rev. Lett.* **77**, 2041 (1996).
- ²⁹A. Gupta, G. Q. Gong, G. Xiao, P. R. Duncombe, P. Lecoeur, P. Trouilloud, Y. Y. Wang, V. P. Dravid, and J. Z. Sun, *Phys. Rev. B* **54**, 15629(R) (1996).
- ³⁰Y. Morimoto, A. Asamitsu, and Y. Tokura, *Phys. Rev. B* **51**, 16491 (1995).
- ³¹A. Tebano, C. Aruta, P. G. Medaglia, F. Tozzi, G. Balestrino, A. A. Sidorenko, G. Allodi, R. De Renzi, G. Ghiringhelli, C. Dallera, L. Braicovich, and N. B. Brookes, *Phys. Rev. B* **74**, 245116 (2006).
- ³²G. Colizzi, A. Filippetti, F. Cossu, and V. Fiorentini, *Phys. Rev. B* **78**, 235122 (2008).
- ³³S. Bueble, K. Knorr, E. Brecht, and W. W. Schmahl, *Surf. Sci.* **400**, 345 (1998).
- ³⁴C. H. Kim, J. W. Jang, S. Y. Cho, I. T. Kim, and K. S. Hong, *Physica B* **262**, 438 (1999).